200 GeV as the momentum increases, whereas the 6- and 8-prong cross sections are almost constant between 70 and 200 GeV. Between 28.5 and 205 GeV, the four-prong cross section falls slowly $(\sim p^{-0.4})$, perhaps indicating the presence of a diffractive component in the four-prong topology.

This experiment was made possible only by the dedicated work of the staff of the National Accelerator Laboratory and the people from Argonne National Laboratory who were responsible for transferring the chamber. To all of them we express our appreciation.

[1]The total corrected number of Dalitz pairs was in reasonable agreement with estimates made of the mean number of π^0's, which in turn was estimated from the number of charged particles. See Ref. 9.

[2]This may be compared with the elastic t dependence of e^{11t} measured by G. Barbiellini et al., Phys. Lett. 39B, 663 (1972).

[3]The total cross section of 38.2 ± 0.2 mb was taken from the compilation of V. Barger and R. J. N. Phillips, Nucl. Phys. B40, 205 (1972). The elastic cross section agrees with 6.8 ± 0.6 mb measured at the intersecting storage rings by M. Holder et al., Phys. Lett. 35B, 361 (1971).

[4]From the design of the beam transport system, one would not expect any substantial hadron or lepton contamination. However, the time structure and instrumentation of the beam did not allow measurement of a possible light-particle contamination. One should then consider the cross sections given in this paper as lower limits.

[5]W. H. Sims et al., Nucl. Phys. B41, 317 (1972).

[6]L. W. Jones et al., Nucl. Phys. B43, 477 (1972).

[7]E. L. Berger, B. Y. Oh, and G. A. Smith, ANL Report No. ANL-HEP 7209, 1972 (to be published).

[8]Soviet-French Collaboration, Mirabelle experiment at 69 GeV/c, February 1972 (unpublished).

[9]The data shown in Fig. 2(a) are for $\langle n_{\pi^0} \rangle$ and come from the work of G. Neuhofer et al. [Phys. Lett. 37B, 438 (1971), and Phys. Lett. 38B, 51 (1972)] who measured the γ rays from pp collisions in the CERN intersecting storage rings. G. R. Charlton and G. H. Thomas [ANL Report No. ANL-HEP 7217, 1972 (to be published)] show that the results are consistent with $\langle n_{\pi^0} \rangle = \frac{1}{2}[\langle n_{\pi^+} \rangle + \langle n_{\pi^-} \rangle]$. If this is combined with the π^+ and π^- measurements from the intersecting storage rings [L. G. Ratner et al., Phys. Rev. Lett. 27, 68 (1971); A. Bertin et al., Phys. Lett. 38B, 260 (1972)], which show $\langle n_{\pi^+} \rangle \simeq \langle n_{\pi^-} \rangle$, one concludes $\langle n_{\pi^-} \rangle \simeq \langle n_{\pi^0} \rangle$.

Parity Violation in Neutron-Capture γ Rays*

J. L. Alberi and Richard Wilson
Department of Physics, Harvard University, Cambridge, Massachusetts 02138

and

I. G. Schröder
Institute for Basic Standards, National Bureau of Standards, Washington, D. C. 20234
(Received 5 July 1972)

We have measured the circular polarization of γ rays from thermal neutron capture in ^{113}Cd and find a $P_\gamma = (6.0 \pm 1.5) \times 10^{-4}$ for the combined 8.51- and 9.04-MeV transitions. This value was measured using a transmission Compton polarimeter and pulse-counting technique. The value confirms the existence of parity-nonconserving terms in the internucleon force.

Several theories of weak interactions suggest that parity-nonconserving effects may be seen in the internucleon force.[1] One such effect is the circular polarization of neutron-capture γ rays. The present experiment measures this effect in the reaction ^{113}Cd$(n, \gamma)^{114}$Cd. Thermal-neutron capture on ^{113}Cd populates a high-energy capture state that is 9.04 MeV above the ground state and has angular momentum and parity $J^p = 1^+$. This excited state decays via a highly complicated series of γ-ray de-excitations.[2] The transition (9.04 MeV) direct to the ground state $(J^p = 0^+)$ and the transition (8.51 MeV) to the first-excited state $(J^p = 2^+)$ are the γ rays expected to exhibit parity-nonconserving effects. In both of these electromagnetic transitions, the predominant parity-allowed transition is magnetic dipole $(M1)$, while any parity-nonconserving admixture to the
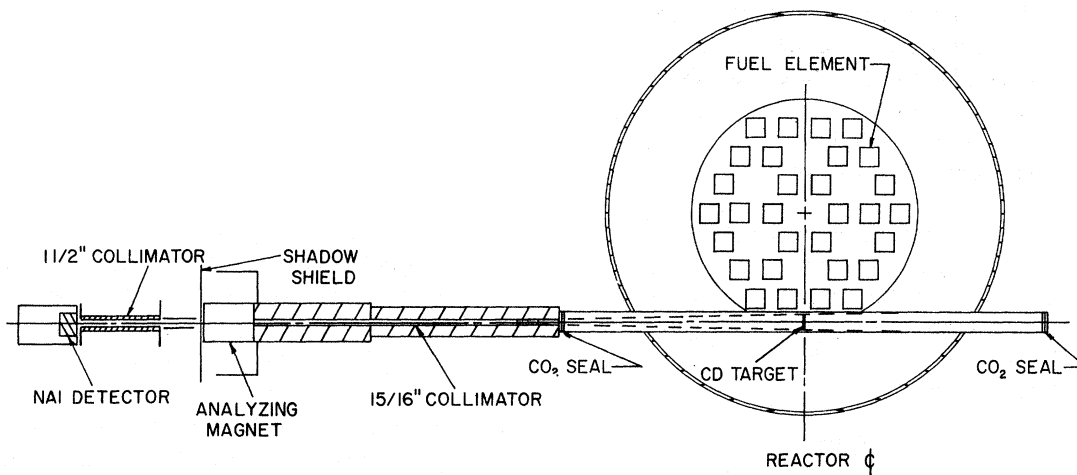
FIG. 1. Schematic diagram of the experimental apparatus at the National Bureau of Standards high-flux reactor.

capture-state wave function (such as mixing of the 1^- giant dipole state) yields an electric dipole ($E1$) transition, which interferes with the magnetic dipole to produce circularly polarized γ rays. Allowed magnetic transition probabilities are less than allowed electric transition probabilities by $(v/c)^2$, where v is the velocity of the nucleons. The relative amplitudes of the weak and strong interactions $\langle V_{wk}/V_{str} \rangle$ is expected to be 10^{-7}. The parity-nonconserving admixture to the capture-state wave function has been calculated[3] to be $\simeq 50\langle V_{wk}/V_{str} \rangle$, and with the enhancement $(c/v)^2$ noted above, the circular polarization is expected to be between 10^{-3} and 10^{-4}.

A schematic diagram of the experiment, performed at the National Bureau of Standards high-flux reactor, is shown in Fig. 1. An elemental Cd target, placed at the center of one of the tangential tubes in the reactor, provided the source of ^{113}Cd capture γ rays. The γ rays from this source, which were overwhelmingly from capture on ^{113}Cd, were collimated by a Bi-Pb collimator designed to view only the target from the detector. All neutrons entering the collimator were stopped by a ^{6}Li absorber. At this point, the γ rays were analyzed by a Compton transmission polarimeter (analyzing magnet in Fig. 1) that converted the circular polarization of the γ beam into a count-rate change by reversing the polarization of the electrons in the iron. (The variation of the γ-ray transmission coefficient is due to the spin-dependent part of the Compton cross section.[4])

The polarimeter was constructed of 0.004-in., high-purity, 3.25%-silicon-iron laminations that reduced the self-time constant of the material

and therefore enabled rapid reversals of electron polarization. The polarimeter had an active length of 17.8 cm and a measured analyzing efficiency ϵ of 6.1% at 9 MeV, i.e., the count rate changed 6.1% for a 100% circularly polarized γ-ray beam.

The beam was detected by a 4 in.×5 in. NaI crystal mounted on an RCA 4522 photomultiplier. This assembly had adequate magnetic shielding to prevent any systematic errors due to influences of the leakage flux from the polarimeter.

The photomultiplier-associated electronics were standard except for the provisions taken to deal with the high overall count rate. The intensities of the 9.04- and 8.51-MeV γ's are 0.26 and 0.46 per 100 captures, respectively. Therefore the overall count rate from the capture γ rays must be several megahertz to achieve a count rate in the 9.04- and 8.51-MeV transitions that will enable the expected effect to be seen in a reasonable length of time. The decay time of the light pulse in NaI is $\simeq 250$ nsec. Such times are clearly too long to prevent pileup and achieve reasonable energy resolution. Clipping the NaI pulse to 80 nsec at the anode of the photomultiplier solves this problem, although this procedure entails some loss of resolution (the resolution at 9.04 MeV is 4.4%). After processing the pulses through a dual discriminator system, however, we were able to achieve a 5-kHz count rate above an 8.0-MeV discriminator threshold. Figure 2 shows the pulse-height spectrum of the three most energetic transitions from the capture state in ^{114}Cd. The straight line is an energy calibration curve. Pileup is less than 15%.

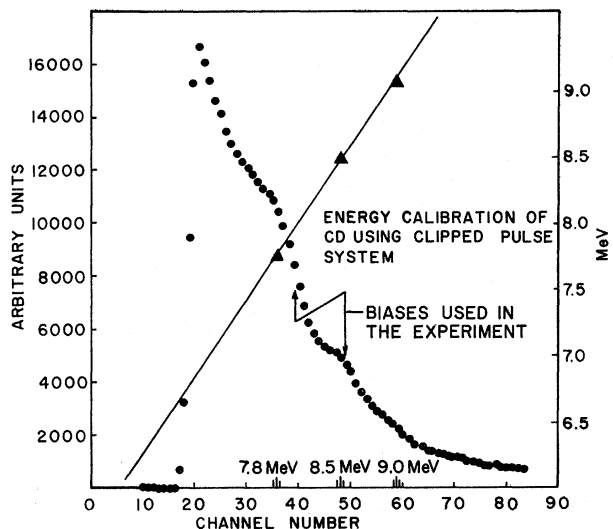A digital switching analyzer was designed and

519

FIG. 2. Energy spectrum of the three most energetic transitions of ^{113}Cd capture γ rays. The straight line is the energy calibration. Statistical errors are smaller than plot symbols.

built to process the discriminator output. This analyzer scaled the output of the integral discriminator, and, at the same time, correlated the direction of analyzing magnet polarization. The input was counted by one 70-MHz scaler for the duration of each counting period, 1 sec, and then was added to one of two registers, depending on the direction of the analyzing-magnet polarization. This method was used to prevent systematic errors arising from the variation of the dead time in the two separate scalers. During reversal of magnet spin polarization, the scaler was gated off to prevent any spurious inductive effects from the magnetic field.

If one denotes by N_1 and N_2 the numbers of counts in the two registers correlated with the di-

rection of the analyzing-magnet polarization, then the count-rate asymmetry δ is defined as

$$\delta = (N_1 - N_2)/(N_1 + N_2),$$

and hence the circular polarization P_γ is

$$P_\gamma = \delta/\epsilon,$$

where ϵ is the analyzing efficiency of the polarimeter as noted above.

Figure 3 illustrates another feature of the switching analyzer. Rather than reversing the electron polarization in the analyzing magnet in a repetitive square-wave pattern as shown for $L = 0$, the more complicated pattern shown for $L = 4$ was used. All the switching patterns shown in this figure have the ability to cancel systematic effects due to nonrandom drifts in count rate to the time dependence shown at the right of the figure. Such nonrandom drifts are caused by temperature fluctuations. However, calculations show that by using the $L = 4$ switching pattern, the effect of such drifts was less than $\delta = 5 \times 10^{-7}$.

Data were taken in a series of runs typically of 12 h duration. At the end of each run, the magnet-current phase was reversed to cancel any possible systematic errors due to the switching-analyzer electronics. None were observed. The data from the individual runs were summed together to give the circular polarization at each energy bias, and random errors were calculated in the usual manner. To insure that the data were not scattering beyond normal statistical fluctuations, χ^2 was calculated for the runs at each energy threshold. No excessive scatter was observed. Control runs were also taken by replacing the Cd target with one of Ti, expected to have no circular polarization. All experimental procedures were followed as with Cd. The energy
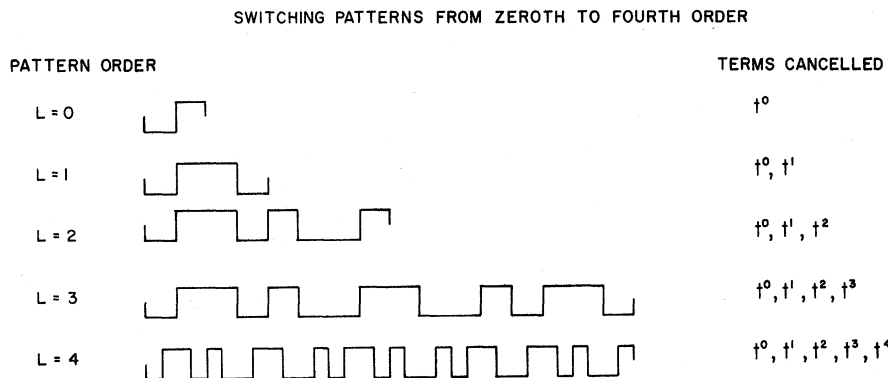

FIG. 3. Magnet-switching waveforms as a function of time. The time scale for the $L = 4$ pattern is compressed by a factor of 2.

TABLE I. Upper limits on systematic errors.

Source	δ
Internal bremsstrahlung	$(4 \pm 6) \times 10^{-7}$
$\vec{\sigma}_e \cdot (\vec{k}_i \times \vec{k}_f)$ Compton term	$< 10^{-7}$
Stray magnetic field	$< 7.5 \times 10^{-7}$
Magnetostriction and self-polarization	$< 10^{-8}$

TABLE II. Results of main and control experiments.

Reaction	Bias (MeV)	δ (10^{-5})	P_γ (10^{-4})
$^{113}Cd(n, \gamma)^{114}Cd$	8.00	3.6 ± 0.90	6.0 ± 1.5
$^{113}Cd(n, \gamma)^{114}Cd$	8.50	6.3 ± 2.6	10 ± 4.2
$^{48}Ti(n, \gamma)^{49}Ti$	6.28	-0.4 ± 0.6	$\cdots$

threshold was set at 6.3 MeV, i.e., at the peak of the dominant γ line. This procedure mimics the rising slope of the Cd energy spectrum.

The upper limit for various systematic effects has been calculated or measured. Table I gives the upper limits on these systematic errors:

(1) Internal bremsstrahlung from the core of the reactor is circularly polarized. The β rays that produce these γ's can range up to 15 MeV, although with ever-decreasing intensity.[5] Therefore, it is possible for the internal bremsstrahlung to scatter from the Cd target in the grazing tube and produce a spurious result. Because the γ collimator is tangential to the reactor core, there is no directly viewed internal bremsstrahlung. Ti was used to measure the amount of internal bremsstrahlung present. The Ti measurement under the conditions described above was 10 times as sensitive to the effect of internal bremsstrahlung as was Cd. Hence we can put an upper limit on the effect of internal bremsstrahlung of $\delta = (4 \pm 6) \times 10^{-7}$.

(2) In lowest-order Compton scattering, there is no term of the form $\vec{\sigma}_e \cdot (\vec{k}_i \times \vec{k}_f)$, where σ_e is the electron spin, and k_i and k_f are the initial and final photon momenta, respectively. This term can influence the count-rate asymmetry by changing the transmission if the apparatus is not totally spatially symmetric. Measuring the possible misalignment in the apparatus calculation[6] gave an upper limit of $\delta = 10^{-7}$.

(3) Stray magnetic fields from the analyzing magnet can induce gain changes in the photomultiplier which, in turn, can produce a spurious count-rate asymmetry. We used measurements of magnetic field extrapolated to the detector position, coupled with measurements of the photomultiplier sensitivity, to calculate the effects of the stray magnetic field. This was measured as $\delta = 7.5 \times 10^{-7}$. The sensitivity of δ to gain change was the same in the Cd runs and the Ti control run; the null effect of the control run was therefore a useful upper limit on the magnetic

field sensitivity of the apparatus.

(4) Magnetostriction and self-polarization in the polarimeter can cause a spurious count-rate asymmetry. This effect, which is proportional to B^2, can be canceled by keeping the difference in magnet current between the two states of the magnet as small as possible. In this case, δ was limited to 10^{-8}. Unannealed silicon iron can have a nonsymmetric saturation flux due to strains. This effect was overcome by choice of magnetic material that had been carefully annealed. Measurements were made of δ as B was changed from 0 to the full value. These agreed with the calculated value and confirmed the analyzing power of the polarimeter.

Table II shows the results of the circular-polarization experiment on ^{113}Cd for two values of discriminator threshold energy as well as the Ti control experiment; the errors quoted are purely statistical. These results are within the range of the estimates quoted above. As can be seen by comparing Tables I and II, the statistical errors are much larger than the systematic errors, and hence the latter can be neglected.

The energy-level scheme is a clear case of vibrational excitation; we hope that the nuclear wave functions can be deduced so that the individual contributions from each transition can be calculated. We gratefully acknowledge the assistance of and helpful discussions with G. Scharff-Goldhaber in the initial stages of this experiment.

[1] E. M. Henley, Annu. Rev. Nucl. Sci. 19, 367 (1969).
[2] G. A. Bartholemew et al., Nucl. Data A5, 1 (1968).
[3] R. J. Blin-Stoyle, Phys. Rev. 120, 181 (1960).
[4] H. Schopper, Nucl. Instrum. Methods 3, 158 (1958).
[5] R. E. Carter, F. Reines, J. J. Wagner, and M. E. Wyman, Phys. Rev. 113, 280 (1959); A. Pythe, Phys. Rev. 107, 1681 (1957).
[6] S. C. Miller and R. M. Wilcox, Phys. Rev. 124, 637 (1961); P. Boek, Phys. Lett. 30B, 628 (1969).